



Full-Field MHz X-ray imaging of laser induced dynamics in liquids

Jozef Haniš, University of Pavol Jozef Šafarik in Košice, Slovakia

Supervised by Dr. Patrik Vagovič,

Center for Free-Electron Laser Science, Hamburg

September 6, 2017

Abstract

X-ray microscopy can reveal the microstructure of opaque material thanks to high penetration power of X-rays. In modern large scale facilities such as synchrotrons and XFELs single X-ray burst can be used to image the structure. In combination with high speed cameras such imaging can fully exploit the frequency of mentioned facilities and X-ray microscopy can be used to image transient processes with exposure given by pulse duration (200 ps down to 10 fs) with Mhz rate sampling frequency. We applied this modality to perform feasibility study of laser induced dynamics in the capillaries containing water. The experiment was performed at ESRF ID19. We succeed to image whole dynamic process using phase contrast mode. We observed the shock wave successive forming of cavitations and formation of high speed water jet (≈ 200 ms). However the signal-to-noise ratio of recorded radiograms is rather low therefore within the scope of this work we explored the contrast enhancement by the single distance phase retrieval technique which led to contrast enhancement of the measured data.

Contents

1	Introduction	3
2	Experimental details	4
3	Image analysis	6
3.1	Single distance phase retrieval	6
3.2	Reconstruction data	8
4	Summary	11

1 Introduction

Fast phenomena in materials generated by external force (high velocity impacts, laser absorption etc.), are of great interest for understanding the physics and behavior of these systems under extreme conditions. For example phenomena like shock-waves and successive thermal heating and expansion in liquid media generated by highly focused laser beams (visible or X-ray) are important for XFEL sample delivery systems.

The samples at XFELs are delivered in liquid jet and the highly focused X-ray pulses are then aligned to hit the sample in the jet. Such interaction can cause strong interaction in the jet which may lead to the destruction of the next coming sample. At European XFEL this problem is even more severe because the X-ray pulses are coming at up to 4.5 MHz rates. This provide 220 ns pulse-to-pulse separation therefore the requirements on jet speeds are more then 100 m/s. It is also not known what is happening with the biological samples if the generated high pressure shock wave wave is hitting the samples. The visible light shadowgraphy [1] is one of the tools to characterize fast processes in liquids, however due to strong scattering of the light on the micro structure (cavitations, micro-bubbles ...) and fluorescence generated just after laser pulse, such samples are not transparent for light probes.

To resolve the structure of above mentioned samples one may use X-ray phase contrast imaging (XPCI) as high penetration power of X-rays allows to reveal the micro structure of non transparent objects. To observe such fast phenomenas propagating through the samples with the speeds of sound in materials MHz rate sampling of the radiograms is necessary. Such sampling at MHz rates can be accomplished at sources such as synchrotrons or European XFEL.

Synchrotrons are in principle large X-ray stroboscopes providing X-ray pulses generated from electron bunches circulating in storage rings. Depending on the filling pattern of storage rings and the circumference of storage rings the the X-ray pulses are generated at MHz down to GHz rates. We used this advantage and constructed pump and probe imaging setup, which we used to image laser induced dynamics of the water in capillaries stimulated by focused laser beam. Whole stochastic process was imaged by X-ray microscope recording at MHz rate. Each frame of the recorded videos was illuminated by X-ray burst coming from single electron bunch passing through the undulator. The experiment was performed at ESRF ID19 beamline.

We recorded phase contrast videos of the water dynamics for various capillary diameters and laser power. Although we can clearly observe the sample structure the signal-to-noise ratio of the XPCI videos is low due to small number of photons contained in single X-ray pulse.

In this work we performed the analysis of experimental data and applied a single distance phase retrieval algorithm to obtain projected sample thickness and the phase, which also led to the contrast increase.

2 Experimental details

The experimental setup has been constructed at ESRF ID19 beamline. We used 16 bunch filling-mode and X-ray central energy of 30 keV provided by tandem undulators using full harmonics. In this filling mode we used the X-ray pulse from each third bunch with 530 ns time separation, due to better synchronization with imaging system. For the illustration various ESRF filling patterns are shown in figure 1.

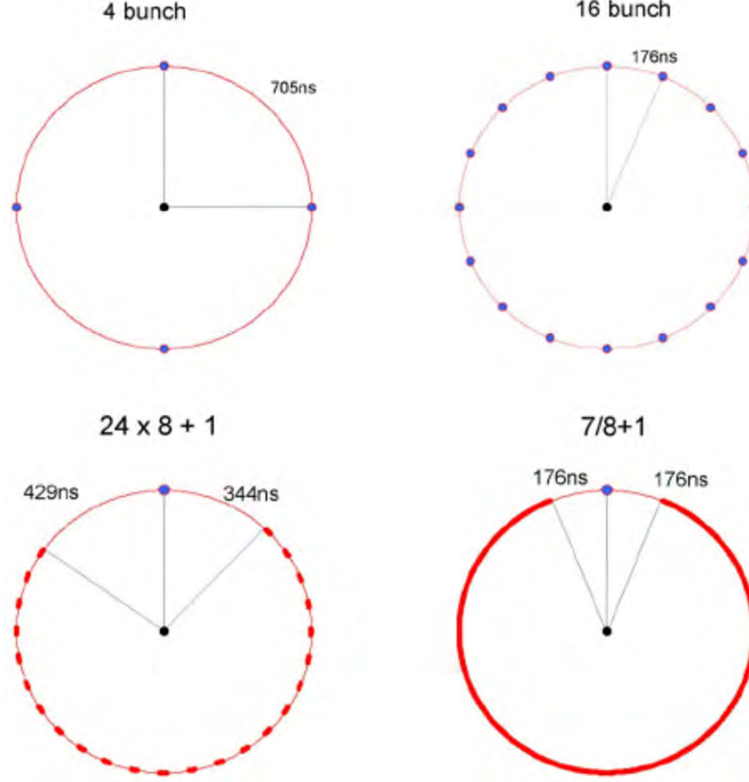


Figure 1: Filling pattern modes at ESRF.

The focused visible laser was illuminating the sample at synchronized 10Hz frequency causing explosions in the water and the full process has been captured using single X-ray pulses using MHz rate X-ray imaging. The X-ray phase contrast imaging mode has been used to visualize the projected density of the sample. The schematics of the experimental arrangement is shown on the figure 2.

The sample examined was water mixed with Nile blue dye contained in the glass capillary. We used several type capillaries with different profiles such as square, rectangular and cylindrical. The internal dimensions of square capillary were $0.4 \text{ mm} \times 0.4 \text{ mm}$, the cylindrical type had three different inner diameters (0.5 mm, 0.75 mm, 1 mm). The reason to use different types of capillaries was to study influence of the shape and dimensions on the dynamical behavior of the water illuminated by highly focused laser pulse.

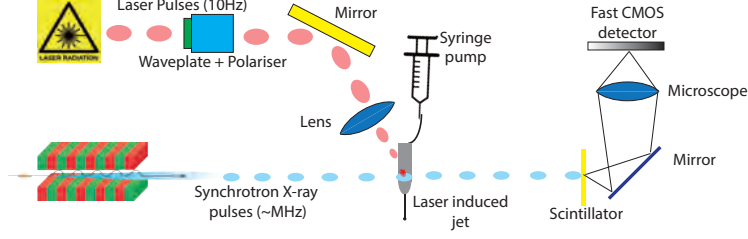


Figure 2: The schematic of the experimental setup

The liquid was stimulated with a focused visible laser (Continuum Minilite) using 355 nm wavelength and measured power of 2.0 mJ, with pulse duration 6-7 ns and spot size $\approx 100 \mu\text{m}$. In some cases, a neutral density filter was used to tune the power to find out optimal power for achieving and explosion in the water.

For fast full-field imaging we used fast CMOS camera Shimadzu HPV-X2 coupled to the optical microscope. X-ray pulses has been converted into visible light with fast decay LYSO:Ce scintillator. If the X-ray pulses are arriving in $\approx 100\text{ns}$ separation time the choice of scintillator is crucial as the fluorescence emission has to diminish before next X-ray pulse is arriving. Photo of the experimental setup is shown in the figure 3 (e).

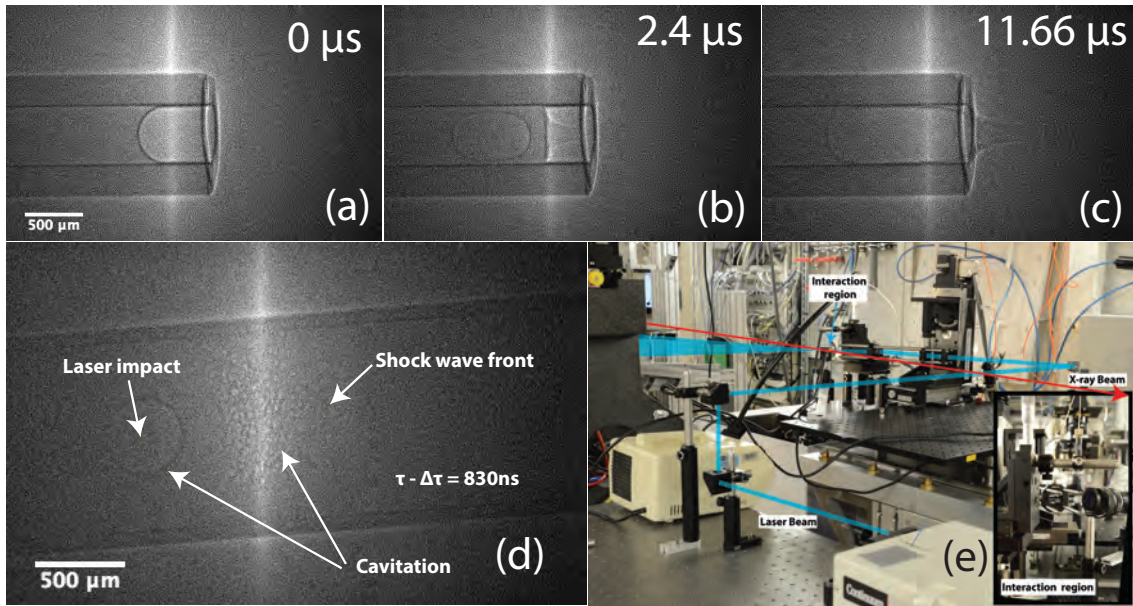


Figure 3: Time evolution of laser induced jet generation event (a,b,c). Observation of shock wave propagating at high speed 1.4 km/s (d) and photo of the setup used for experiment in ESRF ID19 beamline (e).

We found the optimal parameters such as the laser power density and shape of the water-air interface and concentration of dye, as well as the conditions under which the

very repeatable generation of liquid jet has been achieved. The observed speed of jet was ≈ 200 m/s, which makes such jet an promising candidate for the sample delivery at MHz repetition rate XFELs such as European XFEL. Moreover, by the fine time tuning of the pump laser in sheet capillary we observed the evidence of the shockwave propagating at the speed ≈ 1.5 km/s. Although with very weak signal we could see the edge of the shockwave at the distance from the laser impact corresponding to the speed of ≈ 1.4 km/s. Just after the shockwave closer to the impact point we see the generation of micro cavitation indicating that the cause of microcavitation was indeed the shockwave. Such observation was not possible with the visible light imaging because such sample is not transparent and strong fluorescence generated at the impact point prevents such observation of microstructure. The results and experimental setup is shown in figure 3. Although it was not possible with single bunch signal to obtain quantitative information (the projected density) we think it will be possible at European XFEL, where the X-ray pulse contains several orders more photons. Thanks to much higher flux per pulse at European XFEL we can even increase the spatial resolution by using higher magnification.

3 Image analysis

X-ray phase contrast imaging has proven its capability to image the weakly absorbing samples such as polymers or biological tissues with high contrast [2]. In the so called edge regime [3], where the sample is placed at some distance in front of the imaging detector. The density variation within the sample is rendered as intensity oscillations at the imaging plane. This is caused by the refraction of the coherent X-ray beam passing through the sample interfering with unperturbed X-ray beam. To get access to projected sample density a so-called phase retrieval schemes has been developed over the years. In this report we evaluated the single distance phase retrieval method reported by Paganin [4] with normal and reduced filter on obtained X-ray raw radiograms, also modified Bronnikov algorithm [5] too.

3.1 Single distance phase retrieval

The phase-retrieval algorithm, based on the Transport-of-Intensity equation [6], utilizes propagation-based X-ray phase contrast images acquired at a single defocus distance. The method requires a priori knowledge of the complex refractive index for each material present in the sample, together with total projected thickness of the object. With this algorithm we can achieve higher contrast and less noise for measured data and allow us to have a better observation ability to investigate the potency of the above-mentioned phenomena. Thus, the applicability of the algorithms for different imaging situations can be compared in an unbiased way. There are many different phase-retrieval methods that can be applied, we decided to explore the performance of a method for homogeneous object or single material reported by Paganin et. al. and modified Bronnikov algorithm. We used various Fourier filters in single material method for noise suppression. For

Table 1: General pattern for phase retrieval methods

1.	Take a function $g(I)$ of the measured intensity.
2.	Calculate the Fourier transform of $g(I)$.
3.	Multiply by a filter $H(u, v)$ in the frequency domain.
4.	Calculate the inverse Fourier transform to get the filtered quantity g_F

those algorithm, it is assumed that an object consists of a single material, so that phase and absorption are proportional to each other. In the literature the latter effect is often called phase-attenuation duality [7] and we will also refer to those objects as homogeneous objects. If one defines the projected thickness of an object $T(\mathbf{r})$, it is

$$\begin{aligned}\phi(\mathbf{r}) &= -k \int_{-z}^0 \delta(\mathbf{r}') dz = -k\delta T(\mathbf{r}) \\ \mu(\mathbf{r}) &= 2k \int_{-z}^0 \beta(\mathbf{r}') dz = 2k\beta T(\mathbf{r}),\end{aligned}\tag{1}$$

while k is wavenumber defined as $k = \frac{2\pi}{\lambda}$. In this method, we reduced the absorption and phase coefficients β, δ , due to incidence more materials in the observation sample. These coefficients describes refractive index of a material, which is defined as

$$n = 1 - \delta + i\beta.\tag{2}$$

Algorithm for phase-retrieval method is shown in table 1 [7]. Function $g(I)$ is for single material method defined and for modified Bronnikov algorithm as

$$g(I) = \frac{I}{I_0}, \quad g(I) = \frac{I}{I_0} - 1,\tag{3}$$

while I means measurements intensity with sample and I_0 is measurement intensity without sample. $H(u, v)$ means filter function in Fourier domain. For each algorithm is filter $H(u, v)$ defined as

$$H(u, v) = \frac{1}{1 + \frac{\kappa}{4\pi N_F} |\mathbf{k}|^2},\tag{4}$$

$$H(u, v) = \frac{1 + \sigma^2 |\mathbf{k}|^2}{\alpha + \gamma |\mathbf{k}|^2},\tag{5}$$

$$H(u, v) = \frac{1}{\frac{\kappa}{4\pi N_F} + |\mathbf{k}|^2}.\tag{6}$$

Expression 4 describe used filter in single material method, expression 5 describe filter for modified Bronnikov algorithm and expression 6 describe filter used in single material method too, but with different result. Coefficients used in filters are defined, $\kappa = \delta/\beta$,

$N_F = \frac{w^2}{\lambda z}$ is Fresnel number, where λ is wavelength of beam and z is propagation distance, w is half-width and \mathbf{k} is frequency vector in Fourier domain. We have chosen the γ coefficient as the standard deviation divided by mean value and σ coefficient as geometric mean divided by mean value, all these operation was calculated from all reconstruction image after normalization, and α coefficient is calculate as $\alpha = \gamma/\sigma$. For the single material method the final result will be given as phase, also result can be as projected thickness as the sample. Individual algorithm was phase defined as:

$$\phi = \frac{\kappa}{2} \cdot \ln g_F. \quad (7)$$

$$\phi = 2\pi N_F g_F. \quad (8)$$

For single material method with normal and reduced filter the phase map was calculated from expression 7 and for the modified Bronnikov algorithm using expression 8.

3.2 Reconstruction data

The phase-retrieval algorithm requires a priori knowledge about absorption and refraction coefficients δ and β of index of refraction $n = 1 - \delta + \beta i$. Due to the several material which sample contains, glass and water, we choose a refractive index as the difference of the individual refractive indexes. If we label it as absorption and phase coefficient of glass as β_1 and δ_1 , and absorption and phase coefficient of water as β_2 and δ_2 , then the resulting refractive index is in expression 2, while

$$\begin{aligned} \beta &= \beta_1 - \beta_2, \\ \delta &= \delta_1 - \delta_2, \end{aligned} \quad (9)$$

We obtained the coefficients from Henke tables. Individual absorption and refraction coefficients are:

$$\begin{aligned} \beta_1 &= 9,89396 \cdot 10^{-10}, & \delta_1 &= 5,36819 \cdot 10^{-7}, \\ \beta_2 &= 1,074596 \cdot 10^{-10}, & \delta_2 &= 2,58200 \cdot 10^{-7}. \end{aligned} \quad (10)$$

Additional parameters for using single material method are the propagation distance and wavelength. Other parameters required in the phase-retrieval algorithm are propagation distance z , photon energy E and half-width w . These free parameters were set during the experiment:

$$\begin{aligned} z &= 3.171m, \\ E &= 30keV, \\ w &= 8\mu m. \end{aligned} \quad (11)$$

We used the expression 12 to calculate the wavelength $\lambda[\mu m]$.

$$\lambda[\mu m] = \frac{1.2398}{E[eV]}. \quad (12)$$

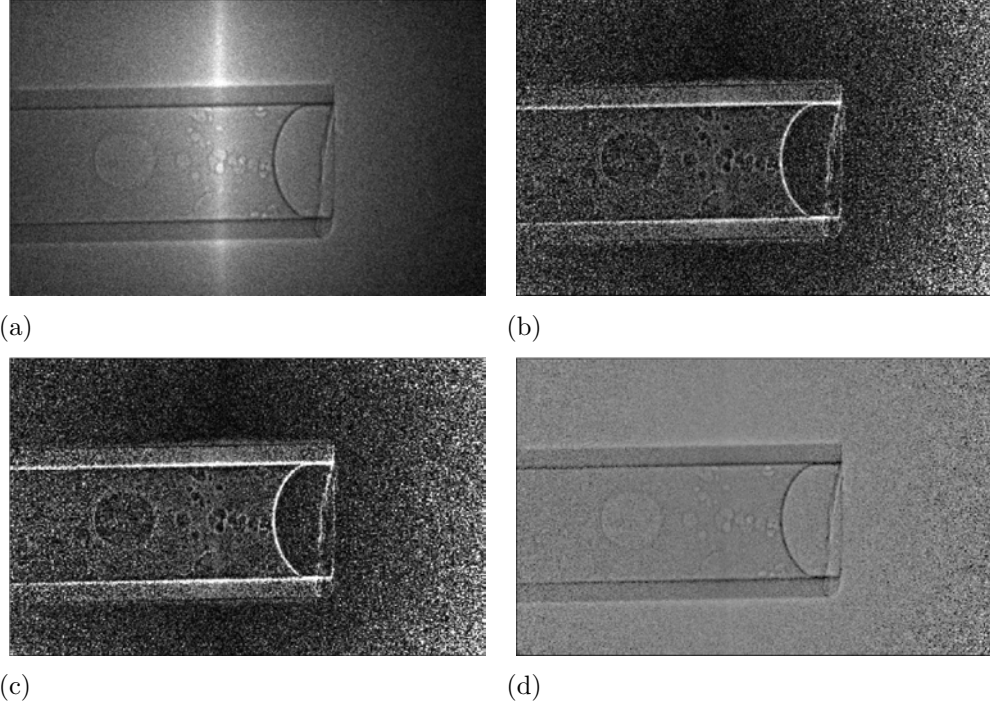


Figure 4: Shown data before and after reconstruction focusing more on bubbles and dynamics in sample, (a): without reconstruction, (b): Modified Bronnikov algorithm, (c): Single material with normal filter, (d): Single material with reduce filter.

Half-width coefficient is determined by real size of one pixel, means $1\text{pix} = 8\mu\text{m}$. The coefficients defined in this way were used to apply the single-material method with normal and reduce filter, also in modified Bronnikov algorithm. The results after reconstruction shown 4 and 5. By comparing the images, we can see that the images in figure 4 (b), (c) are of a similar character to the contrast. Figure 4 (b) is image after application modified Bronnikov algorithm and figure 4 (c) is image reconstruction with single material method. This two filters are better for observation bubbles and dynamics in capillaries. In figure 4, 5 (d) with reduce filter used in single material method have lowest contrast, but the noise is suppress. Reduced single material filter is better utilized to explore dynamics outside capillaries. We applied this algorithms to each image obtained from an experiment with similar result.

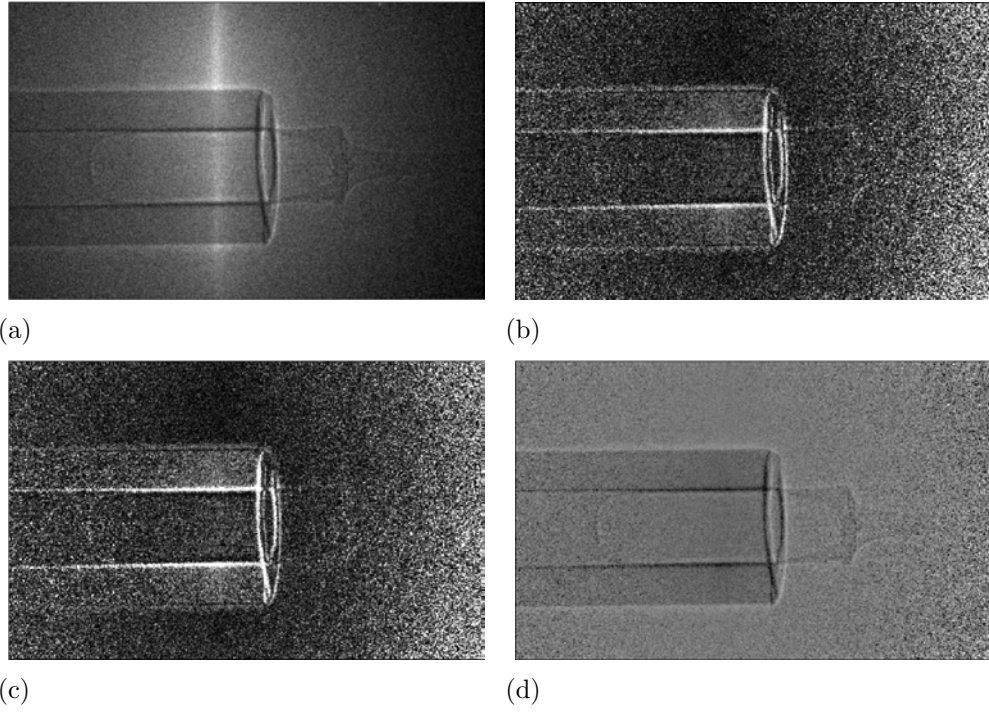


Figure 5: Data before and after reconstruction focusing more on dynamics out of sample, (a): without reconstruction, (b): Modified Bronnikov algorithm, (c): Single material with normal filter, (d): Single material with reduce filter.

4 Summary

In this report, we have examined an experimental data of laser induced dynamics in liquids imaged with MHz rate XPCI technique, which was carried out in the ESRF ID19 beamline. We explored various single distance phase-retrieval methods and applied them to experimental data. By tuning the parameters of the Fourier filters we have been able to optimize contrast for high frequency features and also for density variations within the samples. This work helped us to interpret more clearly the observed fast phenomena.

References

- [1] Gary S Settles. *Schlieren and shadowgraph techniques: visualizing phenomena in transparent media*. Springer Science & Business Media, 2012.
- [2] D. Paganin. *Coherent X-Ray Optics*. Oxford Series on Synchrotron Radiation. OUP Oxford, 2013.
- [3] S.C. Mayo, T.J. Davis, T.E. Gureyev, P.R. Miller, D. Paganin, A. Pogany, A.W. Stevenson, and S.W. Wilkins. X-ray phase-contrast microscopy and microtomography. *Opt. Express*, 11(19):2289–2302, Sep 2003.
- [4] David Paganin, SC Mayo, Tim E Gureyev, Peter R Miller, and Steve W Wilkins. Simultaneous phase and amplitude extraction from a single defocused image of a homogeneous object. *Journal of microscopy*, 206(1):33–40, 2002.
- [5] A Groso, R Abela, and M Stampanoni. Implementation of a fast method for high resolution phase contrast tomography. *Optics express*, 14(18):8103–8110, 2006.
- [6] Keith A. Nugent. X-ray noninterferometric phase imaging: a unified picture. *J. Opt. Soc. Am. A*, 24(2):536–547, Feb 2007.
- [7] Anna Burvall, Ulf Lundström, Per AC Takman, Daniel H Larsson, and Hans M Hertz. Phase retrieval in x-ray phase-contrast imaging suitable for tomography. *Optics express*, 19(11):10359–10376, 2011.